



UNIVERSITY OF LEEDS

This is a repository copy of *An extension to the CAM16 colour appearance model to predict the size effect*.

White Rose Research Online URL for this paper:
<https://eprints.whiterose.ac.uk/170388/>

Version: Accepted Version

Article:

Gao, C, Li, C, Xiao, K orcid.org/0000-0001-7197-7159 et al. (2 more authors) (2021) An extension to the CAM16 colour appearance model to predict the size effect. *Color Research and Application*, 46 (4). pp. 740-748. ISSN 0361-2317

<https://doi.org/10.1002/col.22618>

© 2021 Wiley Periodicals LLC. This is the peer reviewed version of the following article: Gao, C, Li, C, Xiao, K et al. (2 more authors) (2021) An extension to the CAM16 colour appearance model to predict the size effect. *Color Research and Application*, 46 (4). pp. 740-748. ISSN 0361-2317, which has been published in final form at <https://doi.org/10.1002/col.22618>. This article may be used for non-commercial purposes in accordance with Wiley Terms and Conditions for Use of Self-Archived Versions. This article may not be enhanced, enriched or otherwise transformed into a derivative work, without express permission from Wiley or by statutory rights under applicable legislation. Copyright notices must not be removed, obscured or modified. The article must be linked to Wiley's version of record on Wiley Online Library and any embedding, framing or otherwise making available the article or pages thereof by third parties from platforms, services and websites other than Wiley Online Library must be prohibited. Uploaded in accordance with the publisher's self-archiving policy.

Reuse

Items deposited in White Rose Research Online are protected by copyright, with all rights reserved unless indicated otherwise. They may be downloaded and/or printed for private study, or other acts as permitted by national copyright laws. The publisher or other rights holders may allow further reproduction and re-use of the full text version. This is indicated by the licence information on the White Rose Research Online record for the item.

Takedown

If you consider content in White Rose Research Online to be in breach of UK law, please notify us by emailing eprints@whiterose.ac.uk including the URL of the record and the reason for the withdrawal request.



eprints@whiterose.ac.uk
<https://eprints.whiterose.ac.uk/>

An extension to the CAM16 colour appearance model to predict the size effect

Cheng Gao^{1,2}, Changjun Li², Kaida Xiao^{1,3}, Ming Ronnier Luo⁴, Michael R Pointer³

¹ School of Electronics and Information Engineering, University of Science and Technology Liaoning, Anshan 114051, China

² School of Computer and Software Engineering, University of Science and Technology Liaoning, Anshan 114051, China

³ School of Design, University of Leeds, Leeds, UK

⁴ State Key Laboratory of Modern Optical Instrumentation, Zhejiang University, Hangzhou, China

Correspondence

Changjun Li, School of Computer and Software Engineering, University of Science and Technology Liaoning, Anshan, 114051, China. Email: cjliustl@sina.com

Ming Ronnier Luo, State Key Laboratory of Modern Optical Instrumentation, Zhejiang University, Hangzhou, 310058, China. Email: m.r.luo@zju.edu.cn

Abstract

Experience and experimental results show that the perceived colour appearance of an object varies with the size of that object or the viewing angle. Based on available visual size-effect data, it is found that the size effect can be compensated in the CAT16 cone-like space. Furthermore, it is found that, similar to the von Kries chromatic adaptation, size-effect correction can be operated independently on the different cone channels. Hence, the size effect can be easily built into the CAM16 model to predict the colour appearance for stimuli of varying sizes.

KEYWORDS

CAM16, CAT16, color appearance model, cone-like space, size-effect

1. INTRODUCTION

A new colour appearance model, CAM16¹ has recently been proposed which overcomes some of the earlier mathematical problems, and simplifies some of the calculations, in the CIECAM02 model². CIE Technical Committee JTC10³ has recommended that the CAM16 model should replace the CIECAM02 model and be known as the CIECAM16 model. This recommendation is expected to receive final approval in 2021.

Similar to CIECAM02, CAM16 can predict the perceptual attributes, lightness, J , chroma, C , colourfulness, M , brightness, Q , saturation s , hue angle, h and hue quadrature, H , for related colours viewed in the photopic region and over a wide range of viewing conditions. Strictly speaking,

the model can only be used with stimuli with an angular subtense of 2° . Colour appearance however, changes according to the size of the colour stimulus, which is termed the size effect⁴⁻⁷. The common explanation for this effect is that the non-uniform distribution of the photoreceptors (rods and cones) across the human retina leads to colour vision in the peripheral retina being different from colour vision at the fovea. Substantive psychophysical experiments conducted by vision scientists have shown that, when the size of a stimulus is enlarged, the viewing field is extended beyond the central (foveal) region of the retina and that peripheral colour vision deviates from foveal and parafoveal colour vision. These deviations generally increase as the distance of the viewing field from the centre of the retina increases.

1.1 Size effect dataset

The variation in colour appearance as a function of the stimulus size has also been studied by colour scientists⁸⁻¹³. Xiao et al., at the University of Derby¹¹, investigated the effect of stimulus size using two different sets of test stimuli. The first was a 10° painted test stimulus placed in a viewing booth, and the second, the colour of the wall of a room (4 m long x 3 m wide x 3 m high), painted the same colour as the stimulus in the viewing booth, such that the wall subtended approximately 50° at the observer. The walls were lit by lamps placed in the ceiling of the room. In each case the observer had to match a variable 10° colour patch, seen on a computer display, to the colour in the viewing booth or to the colour of the wall of the room. Twelve test colours were used (the room was repainted 12 times), and two light sources (a CIE standard illuminant D65 simulator ($x, y = 0.3143, 0.3312$) and Cool White Fluorescent lamps representing typical office lighting ($x, y = 0.3922, 0.3833$)). The ceiling of the room was painted white and the floor was covered with a mid-grey carpet. All four walls of the room were painted with the same colour. The test stimuli were measured with a portable spectrophotometer and tristimulus values calculated using the CIE 10° standard colorimetric observer and the appropriate illuminant spectral power data.

Ten observers with ages ranging from 20 to 40 years performed the colour matching experiments. In addition to colour matching using the computer display, each observer was asked to select a small chip from an NCS colour atlas that matched each test stimulus. The chips were isolated so that only a single chip could be seen at a time. The colour produced as a match on the computer display was measured using a telespectroradiometer and the appropriate tristimulus values calculated. The CIECAM02 colour appearance model was then used to calculate the corresponding appearance correlates from each set of tristimulus values, leading to an analysis of the colour difference that could be attributed to the different sizes of the stimuli – the 50° wall vs. the 10° colour chip. In general, the results showed that a colour stimulus appeared lighter and more colourful for the larger stimulus size. Stimulus size, however, had no effect on the perception of hue quadrature, H . Figures 1- 3 show the results for lightness, J , chroma, C , and hue quadrature, H , respectively.

Xiao et al.¹², further investigated the effect of stimulus size on colour appearance by using three differently sized sets of test stimuli (2° , 8° and 19°). A variable colour computer display, as described above, was used by ten observers to match 25 colours using a D65 simulator as a light source. In a second experiment 15 colours painted on to cardboard (22° and 44°) were used as test stimuli. The samples were placed on to one wall of the room described above and again, the observers matched each test stimulus using the variable colour computer display. In a third experiment a large LCD TV was used to provide stimuli of two sizes (8° and 50°). The TV had a device white that approximated illuminant D93 ($x, y = 0.2813, 0.2843$). Twelve colours were assessed by each of ten observers.

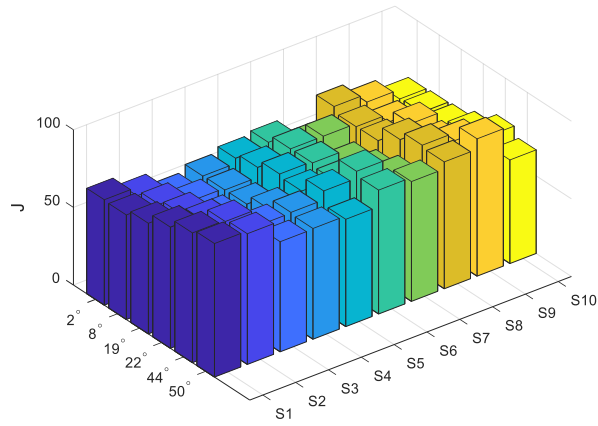


FIGURE 1 Variation in lightness, J , (vertical axis) with the angular subtense of the stimulus, for 10 different colour samples (labelled from S_1 to S_{10})

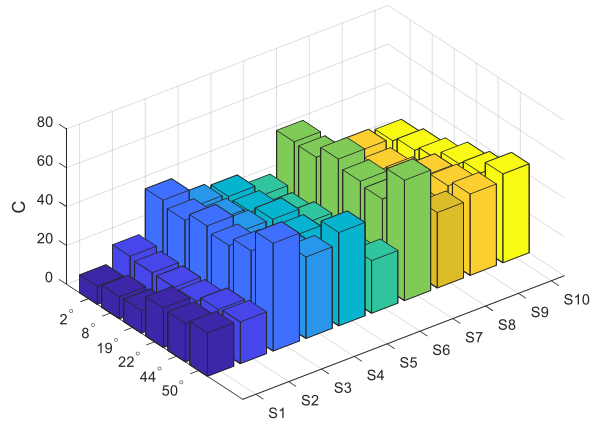


FIGURE 2 Variation in chroma, C , (vertical axis) with the angular subtense of the stimulus, for 10 different colour samples (labelled from S_1 to S_{10})

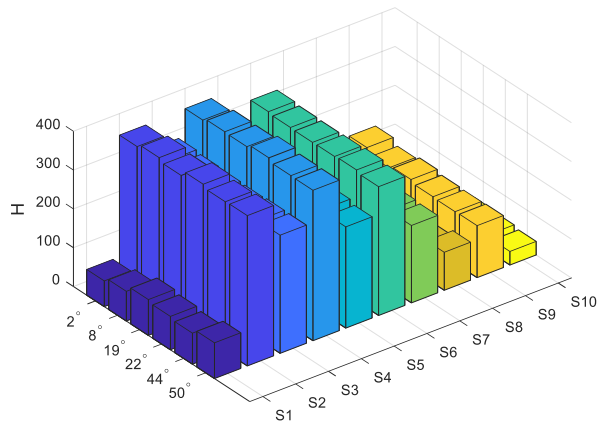


FIGURE 3 Variation in hue quadrature, H , (vertical axis) with the angular subtense of the stimulus, for 10 different colour samples (labelled from S_1 to S_{10})

The six physical sizes in the Xiao et al. experiments¹¹⁻¹³, were categorized into three groups denoted as ‘small-size’, ‘large-size’ and ‘room-size’. The small-size group included the three smaller angular subtenses (2°, 8° and 19°), The large-size group included two of the larger angles (22° and 44°), and the room-size group comprised just one angular subtense, (50°).

Xiao et al.¹³ rescaled the data for the six physical sizes from the experiments described above to form the size effect dataset with 10 colours having six angular subtenses in the range from 2° to 50°, and developed models based on the dataset to transform the colour appearance of a stimulus that has an angular subtense of 2° to that of a stimulus that has any angular subtense in the range from greater than 2° to 50° .

1.2 Available size effect models

Xiao et al. proposed two models^{12,13} to predict the size effect. The first model was a set of two linear equations that modified the CIECAM02 lightness and chroma scales, respectively. Equations (1) and (2) give the modified perceptual lightness, J_θ , and chroma, C_θ , for a larger sized stimulus; J_2 and C_2 are the CIECAM02 lightness and chroma of the stimulus with an angular subtense, θ , of 2°.

$$J_\theta = 100 + K_J(\theta)(J_2 - 100) \quad (1)$$

and

$$C_\theta = K_C(\theta)C_2 \quad (2)$$

where $K_J(\theta)$ and $K_C(\theta)$ are first order polynomials that are functions of the angular subtense of the stimulus, θ . Wei et al.¹⁴ derived improved values versions of the original Xiao et al.¹³ equations:

$$\begin{aligned} K_J(\theta) &= a_J(\theta/2)^2 + b_J(\theta/2) + (1 - a_J - b_J) & \text{for } \theta \geq 2 \\ K_C(\theta) &= a_C(\theta/2)^2 + b_C(\theta/2) + (1 - a_C - b_C) \end{aligned} \quad (3)$$

with $a_J = 0.0000437$, $b_J = -0.01924$, $a_C = 0.000513$, and $b_C = 0.003091$. This model is named the Xiao-SEC model.

Xiao et al.¹³ also derived a model based on a size-effect transform via the cone-like space based on the Hunt-Pointer-Estevéz (HPE) matrix, $\mathbf{M}_{\text{HPE,D65}}$ (normalized relative to the CIE standard illuminant D65)¹⁵.

Let $u_\theta = (X_\theta \ Y_\theta \ Z_\theta)^T$ be the 3-component column vector formed by the tristimulus values of the sample, with angular subtense, θ . The size-effect transform¹³ is then expressed by Equations (4)-(8):

$$\begin{aligned} \alpha_1(\theta) &= 0.000062\theta^2 + 0.00580\theta + 0.5106 \\ \beta_1(\theta) &= 0.000064\theta^2 + 0.00556\theta + 0.5154 \\ \gamma_1(\theta) &= 0.000090\theta^2 + 0.00280\theta + 0.5484 \end{aligned} \quad (4)$$

$$\mathbf{D}_1(\theta) = \begin{pmatrix} \alpha_1(\theta) & 0 & 0 \\ 0 & \beta_1(\theta) & 0 \\ 0 & 0 & \gamma_1(\theta) \end{pmatrix} \quad (5)$$

$$\mathbf{A} = \begin{pmatrix} 1.306 & 0.328 & 0.193 \\ -0.632 & 2.176 & 0.274 \\ -0.543 & 0.047 & 2.241 \end{pmatrix} \quad (6)$$

$$\mathbf{M}_{\text{HPE,D65}} = \begin{pmatrix} 0.400 & 0.708 & -0.081 \\ -2.226 & 1.165 & 0.046 \\ 0.000 & 0.000 & 0.918 \end{pmatrix} \quad (7)$$

$$u_{\theta,P} = \mathbf{M}_{\text{HPE,D65}}^{-1} \mathbf{AD}_1(\theta) \mathbf{M}_{\text{HPE,D65}} u_2 \quad (8)$$

Note that subscript P , in $u_{\theta,P}$ in Equation (8), denotes the prediction to the visual result u_θ . The matrix $\mathbf{M}_{\text{HPE,D65}} u_2$ can be considered as the cone-like response transformed from CIE XYZ tristimulus space, hence Equation (8) has the form of a "chromatic adaptation transform"¹⁶. Since the matrix $\mathbf{AD}_1(\theta)$ is a full 3 by 3 matrix however, the size-effect transform makes the corrections using all three channel signals in the HPE cone-like space. Furthermore, $\mathbf{AD}_1(2)$ is a full matrix that is different from the identity matrix, and therefore the correction is made even when the size of the stimulus has an angular subtense of 2° , which might seem unreasonable. This size-effect transform model is named the Xiao-SET model.

Both the Xiao-SEC and Xiao-SET models were proposed to be used with the CIECAM02 colour appearance model, and Xiao et al.¹³ showed that the Xiao-SET model performed better than the Xiao-SEC model. Since the $\mathbf{M}_{\text{HPE,D65}} u_2$ space used in the Xiao-SET model is different from the $\mathbf{M}_{02} u_2$ space used in the CIECAM02 model, however, in order to predict the colour appearance of a stimulus with an angular subtense, θ , from the tristimulus values, u_2 , of the same sample with an angular subtense of 2° , the tristimulus values, $u_{\theta,P}$, must be computed using Equation (8), and $u_{\theta,P}$ becomes the input to the CIECAM02 model. Thus, this conflict means that it is not straight-forward to use the Xiao-SET model with the CIECAM02 appearance model.

In this paper, the size-effect correction is investigated using the CAT16 cone-like space¹. It was found that the size effect can be corrected in this space and the correction can be made independently on each of the CAT16 cone-like channels. The correction factor for each channel is an increasing function of the stimulus size or angular subtense. The proposed size-effect correction model is a von Kries type of chromatic adaptation transform for size-effect correction. Furthermore, unlike the Xiao-SET model, the proposed new model can be easily and economically (in terms of computational cost) added to CAM16 appearance model.

2. Size Correction in CAT16 Cone-like Space

The CAT16 cone-like space¹ is used in the CAM16 colour appearance model and has been shown to be an improvement of the earlier Hunt-Pointer-Estevéz (HPE) cone-like space^{15,17}. Hence, CAT16 cone-like space is the preferred space for appearance models.

If \mathbf{M}_{16} is the CAT16 matrix¹, the CIE XYZ tristimulus can be transformed to CAT16 cone-like space using Equation (9):

$$\begin{pmatrix} R_2 \\ G_2 \\ B_2 \end{pmatrix} = \mathbf{M}_{16} \begin{pmatrix} X_2 \\ Y_2 \\ Z_2 \end{pmatrix} \quad (9)$$

Based on the Xiao-SET model¹³, and the von Kries type transform for chromatic adaptation, the proposed size correction can be carried out independently for each channel from 2° to θ° ($\theta < 50^\circ$) in CAT16 cone-like space using Equation (10):

$$\begin{pmatrix} R_\theta \\ G_\theta \\ B_\theta \end{pmatrix} = \begin{pmatrix} \alpha(\theta)R_2 \\ \beta(\theta)G_2 \\ \gamma(\theta)B_2 \end{pmatrix} = \begin{pmatrix} \alpha(\theta) & 0 & 0 \\ 0 & \beta(\theta) & 0 \\ 0 & 0 & \gamma(\theta) \end{pmatrix} \begin{pmatrix} R_2 \\ G_2 \\ B_2 \end{pmatrix} = \mathbf{D}(\theta) \begin{pmatrix} R_2 \\ G_2 \\ B_2 \end{pmatrix} \quad (10)$$

Here, $\alpha(\theta)$, $\beta(\theta)$, and $\gamma(\theta)$ are functions of the viewing angle θ , and $\mathbf{D}(\theta)$ is a 3 by 3 diagonal matrix formed by the size correction factors $\alpha(\theta)$, $\beta(\theta)$, and $\gamma(\theta)$. Combining Equations (9) and (10) results in the following equation linking the tristimulus values for a stimulus with an angular subtense of 2° to those for θ° :

$$u_{\theta,P} = \mathbf{M}_{16}^{-1} \mathbf{D}(\theta) \mathbf{M}_{16} u_{2^\circ} \quad (11)$$

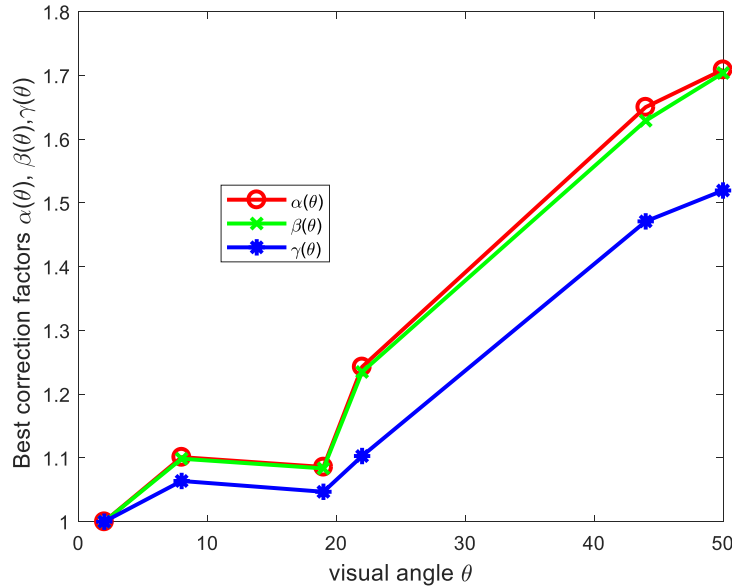


FIGURE 4 The best size-correction factors, $\alpha(\theta)$, (red circle), $\beta(\theta)$, (green cross), $\gamma(\theta)$, (blue asterisk), versus the angular subtense, θ , using piecewise linear interpolation

Note that Equation (11) has the form of a von Kries chromatic adaptation transform¹⁶ and is similar to, but simpler than, Equation (8). The best values for the correction factors $\alpha(\theta)$, $\beta(\theta)$, and $\gamma(\theta)$ can be obtained by minimizing the difference between $u_{\theta,P}$ and u_θ by using the least squares method in either tristimulus space or CIELAB colour-difference space. Analysis using the data from Xiao et al.¹¹ showed that minimization in terms of CIELAB colour-difference between $u_{\theta,P}$ and u_θ gave the best results and thus the best correction factors $\alpha(\theta)$, $\beta(\theta)$, and $\gamma(\theta)$, and the values are

listed in Table 1. Figure 4 shows the variations of the factors $\alpha(\theta)$ (red circle), $\beta(\theta)$ (green cross), and $\gamma(\theta)$ (blue asterisk) with the angular subtense, θ , respectively. It can be seen that, in general, the factors increase with increase in the angular subtense except for angular subtense at 22° . The best correction factors in the red and green channels are approximately equal, while those in the blue channel are slightly lower. Table 2 shows the performance of the size effect corrections using Equation (11) in terms of the average (Ave), maximum (Max) and median (Med) CIELAB colour-difference, together with the colour difference without the size effect corrections. The data show that, as the angular subtense increases, the colour difference increases, which clearly demonstrates the size effect. Columns 5-7 show the colour difference between u_θ and $u_{\theta,P}$ using the proposed size effect correction, Equation (11) and it can be seen that improvements are achieved, although the gain is less for 8° than for the other viewing angles.

TABLE 1 Scaling factors $\alpha(\theta)$, $\beta(\theta)$, $\gamma(\theta)$ obtained by minimizing the CIELAB colour-difference between the matrices $u_{\theta,P}$ and u_θ

| θ | 2° | 8° | 19° | 22° | 44° | 50° |
|------------------|-----------|-----------|------------|------------|------------|------------|
| $\alpha(\theta)$ | 1 | 1.101213 | 1.085767 | 1.242813 | 1.650306 | 1.709043 |
| $\beta(\theta)$ | 1 | 1.098735 | 1.083536 | 1.234871 | 1.629003 | 1.703887 |
| $\gamma(\theta)$ | 1 | 1.063835 | 1.046851 | 1.102975 | 1.471095 | 1.519538 |

TABLE 2 The performance of the size effect corrections using Equation (11) and Equation (8) in terms of the average (Ave), maximum (Max) and median (Med) CIELAB colour difference between stimuli without correction and with size-effect correction.

| θ | Without correction | | | With corrections using Equation (11) | | |
|------------|--------------------|-------------|-------------|--------------------------------------|------------|------------|
| | Ave | Max | Med | Ave | Max | Med |
| 8° | 5.2 | 14.1 | 4.1 | 4.5 | 12.2 | 3.2 |
| 19° | 6.0 | 8.7 | 5.5 | 4.4 | 6.3 | 4.3 |
| 22° | 11.1 | 15.2 | 11.9 | 5.1 | 6.7 | 5.3 |
| 44° | 17.3 | 18.9 | 18.0 | 5.5 | 7.3 | 5.3 |
| 50° | 20.8 | 28.5 | 20.1 | 10.6 | 15.1 | 10.1 |
| Mean | 12.1 | 17.1 | 11.9 | 6.0 | 9.5 | 5.6 |

3. Modelling the size correction factors $\alpha(\theta)$, $\beta(\theta)$, $\gamma(\theta)$

Figure 4 also shows the piecewise linear interpolations for the size correction factors $\alpha(\theta)$ (red line), $\beta(\theta)$ (green line), $\gamma(\theta)$ (blue line). It might be appropriate however, if they could be modelled as "smooth" functions of the angular subtense. To this end, it can be seen that the optimum values for $\alpha(\theta)$ and $\beta(\theta)$ with angular subtense of 19° deviate markedly from their closest size value, i.e. from the 22° values, while the other values for $\alpha(\theta)$ and $\beta(\theta)$, with angular subtense of 2° , 8° , 22° , 44° and 50° respectively, closely follow a straight line (a first order polynomial function). Furthermore, if the data with angular subtense of 19° is omitted, the remaining $\gamma(\theta)$ values can be fitted with a

second order polynomial. Based on the above observation, the data with angular subtense of 19° was omitted from further analysis and the size correction factors $\alpha(\theta)$, $\beta(\theta)$, $\gamma(\theta)$ were modelled as first and second order polynomials of the angular subtense to give the general expressions given by Equations (12) and (13) respectively:

$$g(\theta) = 1 + c_1(\theta - 2) \quad (12)$$

$$f(\theta) = 1 + (\theta - 2)(c_2 + c_3\theta) / 1000 \quad (13)$$

The coefficients c_1 , c_2 and c_3 are given in Table 3 for each of the three size correction factors $\alpha(\theta)$, $\beta(\theta)$, $\gamma(\theta)$ respectively. Figures 5-7 shows the best (circle), first order (solid line) and second order (dotted line) polynomials for the size correction factors $\alpha(\theta)$, $\beta(\theta)$, and $\gamma(\theta)$ respectively. It can be seen from Figures 5 and 6, that the first and second order polynomials are similar. Hence, the first order polynomial was selected for $\alpha(\theta)$ and $\beta(\theta)$. For $\gamma(\theta)$ however, Figure 7, it can be seen that first and second polynomials are rather different and it was found that the second order polynomial performed better than first order polynomial model. Hence the second order polynomial was selected for $\gamma(\theta)$. The performance of the proposed size-effect corrections using Equations (12) for $\alpha(\theta)$ and $\beta(\theta)$ and Equation (13) for $\gamma(\theta)$, with the coefficients given in Table 3, in terms of the average (Ave), maximum (Max) and median (Med) CIELAB colour-differences, are given in Table 4 (columns 2-4). In the last row of Table 4, the overall mean values of the average, maximum and median colour differences, for all angular subtenses from 8° to 50° (omitting 19°), are seen to be 6.6, 10.8 and 6.6 CIELAB colour-difference units respectively, which are slightly worse than the values, 6.4, 10.3, and 6.0, for the overall means for the best size correction results (without the 19° data) in columns 5-7 of Table 2. The last three columns in the Table 4 show the performance of the Xiao-SET model and it can be seen that the Xiao-SET model performs better in terms of average and median colour differences. However, the Xiao-SET model has prediction errors even for the 2° angular subtense while the proposed model does not.

TABLE 3 The coefficients, c_1 , c_2 and c_3 , for each channel for the size-correction factors using Equations (12) and (13).

| | c_1 | c_2 | c_3 |
|------------------|----------|----------|----------|
| $\alpha(\theta)$ | 0.013842 | 12.91498 | 0.016193 |
| $\beta(\theta)$ | 0.013602 | 11.99885 | 0.032043 |
| $\gamma(\theta)$ | 0.010439 | 3.961454 | 0.145073 |

TABLE 4 The performance of the proposed size-effect correction method (with correction factors using Equation (12) for $\alpha(\theta)$ and $\beta(\theta)$ and Equation(13) for $\gamma(\theta)$, and coefficients in Table 3), together with the Xiao-SET model, in terms of the average (Ave), maximum (Max) and median (Med) CIELAB colour-difference

| θ | The proposed method | | | Xiao-SET (Using Equation (8)) | | |
|----------|---------------------|------|-----|-------------------------------|------|-----|
| | Ave | Max | Med | Ave | Max | Med |
| 2° | 0 | 0 | 0 | 2.9 | 5.5 | 3.1 |
| 8° | 4.5 | 12.8 | 3.1 | 4.5 | 13.3 | 3.4 |
| 22° | 5.1 | 7.6 | 5.4 | 4.6 | 7.9 | 4.6 |

| | | | | | | |
|------|------------|-------------|------------|------------|-------------|------------|
| 44° | 5.7 | 7.6 | 6 | 3.0 | 6.8 | 2.7 |
| 50° | 10.9 | 15.4 | 11.9 | 8.3 | 15.1 | 7.8 |
| Mean | 6.6 | 10.8 | 6.6 | 5.1 | 10.8 | 4.6 |

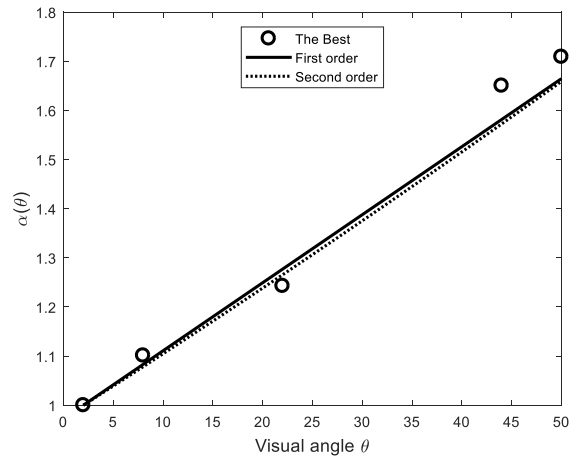


FIGURE 5 The first order (solid line), and second order (dotted line) polynomials for the red channel for size-correction factor, $\alpha(\theta)$

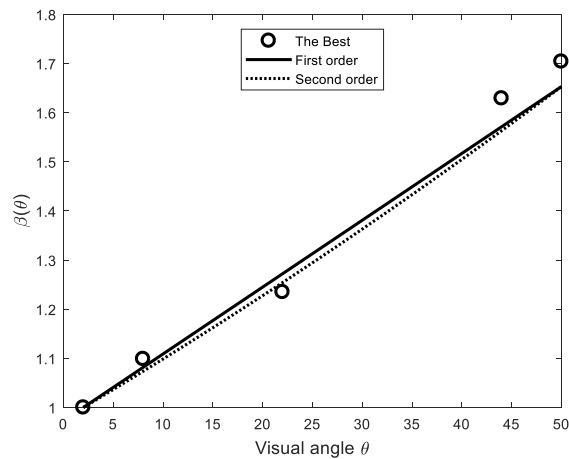


FIGURE 6 The first order (solid line), and second order (dotted line) polynomials for the green channel for size-correction factor, $\beta(\theta)$

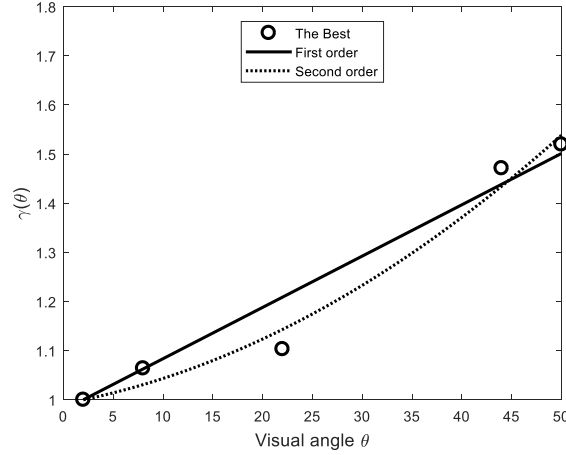


FIGURE 7 The first order (solid line), and second order (dotted line) polynomials for the blue channel for size-correction factor, $\gamma(\theta)$

4. Extension of the CAM16 for the size-effect prediction

Since the CAT16 transform is part of the CAM16 model, and the proposed size-effect corrections are also based on the CAT16 cone-like space, the matrix is used for both size-effect correction and chromatic adaptation. Thus, CAM16 can be easily extended for to predict the size effect with very little extra time required to compute the size-correction factors $\alpha(\theta)$, $\beta(\theta)$, $\gamma(\theta)$ using either the first or second order polynomial at the given angular subtense, θ , and making the corrections in CAT16 cone-like space using Equation (10). Thus, the size-effect prediction using the CAM16 model can be completed with minor changes to the chromatic adaptation stage. Step 2 for the calculating the effect of chromatic adaptation in the CAT16 cone-like space in the calculation of the CAM16 forward model, given in the appendix of the paper by Li et al.¹, is given below:

Step 2: Complete the colour adaptation of the illuminant in the corresponding cone response space

$$\begin{pmatrix} R_c \\ G_c \\ B_c \end{pmatrix} = \begin{pmatrix} D_R \cdot R \\ D_G \cdot G \\ D_B \cdot B \end{pmatrix} \quad (14)$$

Note that all symbols here have the same meaning as in the CAM16 paper¹. D_R , D_G , and D_B are chromatic adaptation factors computed in Step 0, and R, G, B are cone-like response signals transformed from TSV of 2° stimulus using Equation (9).

For predicting the size effect for stimuli and an angular subtense, θ , Step 2 can be changed to:

Step 2': Complete the colour adaptation of the illuminant in the corresponding cone response space and the size-effect correction for stimuli with viewing angle, θ :

$$\begin{pmatrix} R_c \\ G_c \\ B_c \end{pmatrix} = \begin{pmatrix} \alpha(\theta) \cdot D_R \cdot R \\ \beta(\theta) \cdot D_G \cdot G \\ \gamma(\theta) \cdot D_B \cdot B \end{pmatrix} \quad (15)$$

Here, size-correction factors $\alpha(\theta)$ and $\beta(\theta)$ are the first order polynomials defined by Equation (12), and $\gamma(\theta)$ is the second order polynomial defined by Equation (13), and the values of the coefficients are given in Table 3.

Thus, the extended CAM16 model, which is the same as the original CAM16 model¹ except the revised Step 2 above, can predict the effect of different sized stimuli. Table 5 (columns 5-7) summarizes the performance of the revised model using the Xiao et al. data^{11,12}, in terms of the Coefficient of Variation (CV), together with data without the size-effect correction (columns 2-4). It can be seen that the extended CAM16 model successfully makes the size-effect corrections.

Table 6 shows the performance of the Xiao-SEC and Xiao-SET models. Compared with the results in Table 5, the models perform the same for predicting lightness. For predicting the hue quadrature, the extended CAM16 and Xiao-SET perform equally well and they are better than the Xiao-SEC model. For predicting chroma, the Xiao-SET model is the best and the extended CAM16 is better than the Xiao-SEC model. Overall, the Xiao-SET model is the best, and the proposed model is the second best. The proposed model, however, is simpler and is similar to the von Kries type of chromatic adaptation transform. In addition, the Xiao-SET model is not as convenient for application with the CIECAM02 and CAM16 models. Furthermore, the Xiao-SET model makes corrections when the angular subtense, θ , is equal to 2° , which is incorrect.

TABLE 5 The performance (CV) of the extended CAM16 model for predicting the size effect together with data without size effect correction

| θ | Without size effect corrections | | | Extended CAM16 model | | |
|------------|---------------------------------|-----------|----------|----------------------|-----------|----------|
| | J | C | H | J | C | H |
| 8° | 9 | 6 | 3 | 8 | 6 | 3 |
| 22° | 11 | 20 | 6 | 5 | 11 | 3 |
| 44° | 20 | 19 | 4 | 4 | 12 | 3 |
| 50° | 21 | 15 | 6 | 8 | 11 | 4 |
| Mean | 15 | 15 | 5 | 6 | 10 | 3 |

TABLE 6 The performance (CV) of the Xiao-SEC and Xiao-SET models for predicting the size effect

| θ | Xiao-SEC | | | Xiao-SET | | |
|------------|----------|-----------|----------|----------|----------|----------|
| | J | C | H | J | C | H |
| 2° | - | - | - | 3 | 5 | 2 |
| 8° | 8 | 6 | 3 | 7 | 6 | 3 |
| 22° | 4 | 20 | 6 | 5 | 9 | 2 |
| 44° | 4 | 20 | 4 | 3 | 7 | 2 |
| 50° | 8 | 15 | 5 | 8 | 8 | 3 |
| Mean | 6 | 15 | 5 | 6 | 8 | 3 |

5. CONCLUSION

This paper describes an extension of the CAM16 colour appearance model to predict the effect on the appearance of stimuli with different values of angular subtense. It was found that the size-effect correction can be modelled as a von Kries type of chromatic adaptation transform with different scaling factors. The tristimulus values, $X_\theta, Y_\theta, Z_\theta$ of a stimulus with angular subtense, θ , that is different

from 2° can be transformed to the CAT16 cone-like space via the CAT16 matrix (Equation (9)) to derive cone response signals $R_\theta, G_\theta, B_\theta$. It was first found that these cone response signals can be obtained by adjusting the cone response signals for a 2° stimulus, R_2, G_2, B_2 independently, i.e., $R_\theta = \alpha(\theta)R_2$, $G_\theta = \beta(\theta)G_2$, and $B_\theta = \gamma(\theta)B_2$. The size-correction factors $\alpha(\theta), \beta(\theta), \gamma(\theta)$ were observed to increase generally with increasing angular subtense, θ , and finally factors $\alpha(\theta)$ and $\beta(\theta)$ were modelled as first order polynomials defined by Equation (12), and $\gamma(\theta)$ was modelled as a second order polynomial defined by Equation (13) and all coefficients are given in Table 3. Thus, the size-effect correction can be modelled as a transform: $u_{\theta,P} = M_{16}^{-1}D(\theta)M_{16}u_2$ (Equation (10)), which is similar to a von Kries type of chromatic adaptation transform but with different scaling factors. Since the matrix transforming the XYZ tristimulus space to cone-like space is the CAT16 matrix, the size-effect correction can easily be added to the CAM16 model. The performance of the extended CAM16 model was tested using the Xiao dataset and it was found that the proposed model was better than the Xiao-SEC model, but worse than the Xiao-SET model. The Xiao-SET model however, is cannot easily be added to the CAM16 model and thus hence the proposed model is recommended for the size-effect correction.

Funding information

National Natural Science Foundation of China (Grant numbers: 61575090, 61775169, 61775190). Liaoning Natural Science Foundation (2019-ZD-0267), and Scientific Research Project of Liaoning Educational Department (2020LNJC01).

ORCID

Changjun Li <https://orcid.org/0000-0002-9942-7690>

Cheng Gao <https://orcid.org/0000-0003-2233-2914>

Data Availability Statement

The data used to support the findings of this study are available from the corresponding author upon request. The data are not publicly available due to privacy restrictions.

REFERENCES

- [1] Li CJ, Li ZQ, Wang ZF, Xu Y, Luo MR, Cui G, Melgosa M, Brill MH, Pointer MR. Comprehensive color solutions: CAM16, CAT16 and CAM16-UCS. *Color Research & Application*. 2017; 42: 703–718 .
- [2] CIE 159:2004. A colour appearance model for colour management systems: CIECAM02. Vienna: CIE; 2004.
- [3] CIE JTC10 Technical Report, draft version 8, 2020.
- [4] Wyszecki GW, Stiles WS. *Color Science: Concepts and Methods, Quantitative Data and Formulae*, 2nd edition. New York: Wiley; 2000.
- [5] Stabell B, Stabell U. Color vision in the peripheral retina under photopic conditions. *Vision Research*. 1982; 22(7): 839–844.
- [6] Stabell U, Stabell B. Rod-cone color mixture: Effect of size and exposure time. *Journal of the Optical Society of America A Optics Image ence & Vision*. 1999; 16(11): 2638–2642.
- [7] Nerger JL, Volbrcht VJ, Ayde CJ. Unique hue judgment as a function of test size in the fovea and at 20-deg temporal eccentricity. *Journal of the Optical Society of America A Optics Image ence & Vision*. 1995; 12(6): 1225–1232.

- [8] Kutas G, Gocza K, Bodrogi P, Schanda J. Color size effect. In: Proceedings of the 2nd European Conference on Color in Graphics Imaging and Vision. Aachen. 2004; 70–73.
- [9] Kutas G, Bodrogi P. Color appearance of large homogenous visual field. *Color Research Application*. 2010; 33(1): 45–54.
- [10] Hsieh T, Chen I. Area-dependent colour appearance shift. In: Proceedings of the 10th Congress of the International Colour Association. Granada. 2005; 1115–1118.
- [11] Xiao KD, Luo MR, Li CJ, Hong GW. Colour appearance of room colours. *Color Research & Application*. 2010; 35(4): 284-293.
- [12] Xiao KD, Luo MR, Li CJ, Cui GH and Park D. Investigation of colour size effect for colour appearance assessment. *Color Research & Application*. 2011; 36(3): 201-209.
- [13] Xiao KD, Luo MR, and Li CJ. Color size effect modeling. *Color Research & Application*. 2012; 37: 4-12.
- [14] Wei ST, Luo MR, Xiao KD. A comprehensive model of colour appearance for related and unrelated colours of varying size viewed under mesopic to photopic conditions. *Color Research & Application*. 2017; 42 (3): 293-304.
- [15] Hunt RWG, Pointer MR. A colour appearance transform for the CIE 1931 standard colorimetric observer. *Color Research & Application*. 1985; 10: 165–179.
- [16] Gao C, Wang ZF, Xu Y, Melgosa M, Xiao KD, Brill MH, Li CJ. The von Kries chromatic adaptation transform and its generalization. *Chinese Optics Letters*. 2020; 18(3): 33301.
- [17] Estevez O. On the fundamental data base of normal and dichromatic vision. PhD thesis. University of Amsterdam. The Netherlands. 1979.